Neutron capture cross sections of ^{184,189,190,192}Os and the decays of ^{185}Os,^{190}Os^{m}, ^{191}Os, and ^{193}Os

K. S. Krane
Department of Physics, Oregon State University, Corvallis, Oregon 97331, USA
(Received 20 February 2012; published 23 April 2012)

Radiative neutron capture cross sections have been measured for the stable isotopes of natural Os with mass numbers 184, 189, 190, and 192 by observing radioactive decays of the activation products following neutron irradiation of naturally occurring Os. From irradiations of Os samples separately with thermal and epithermal neutrons, independent values of the thermal cross sections and resonance integrals have been deduced. By observing the γ rays emitted by the activation products ^{185}Os, ^{190}Os^{m}, ^{191}Os, and ^{193}Os, improved values for the energies and intensities of the γ rays and the decay half-lives have been obtained, enabling corresponding improvements in the energy values and β-decay feedings of levels in the daughter nuclei.

DOI: 10.1103/PhysRevC.85.044319 PACS number(s): 25.40.Lw, 27.70.+q, 27.80.+w, 23.20.Lv

I. INTRODUCTION

The neutron capture cross sections of the stable naturally occurring Os nuclides (A = 184, 189, 190, 192) that produce radioactive isotopes pose an interesting set whose measurements offer challenges to the experimenter. Based on previously measured values (as summarized by Mughabghab [1] and tabulated by the National Nuclear Data Center [2]), it is known that the Os thermal capture cross sections range from about 3000 b for the neutron-deficient and rare isotope ^{184}Os to less than a mb for captures by the abundant ^{189}Os isotope leading to ^{190}Os^{m}. The case of ^{184}Os is one of very few nuclei for which the resonance integral is smaller than the thermal cross section. The unusually small thermal cross section for production of ^{190}Os^{m} results from the large spin change between the capturing state (3/2) and the isomer (10). Capture by ^{190}Os produces both the isomer and the ground state in ^{191}Os; because the spin change for production of the isomer is smaller than that of the ground state (3/2 vs 9/2), the isomer is produced in greater quantities. The isomer decays only to the ground state but unfortunately does so through a highly converted 74 keV transition whose small γ-ray intensity (less than 0.1%) is unobservable amidst the background of intense x-rays produced in the Os decays. Thus the decay of the isomer can be observed in γ-ray emissions only indirectly through the growth and decay of the ground-state activity, which complicates the extraction of the cross sections of both the isomer and the ground state.

Partly as a result of these experimental difficulties, there is a large variation among the previously measured values of the Os cross sections. The previously reported values of the ^{189}Os cross section differ by more than an order of magnitude, and there is no clear consensus among the previous measurements of the ^{190}Os cross sections. Even in the case of capture by ^{192}Os to ^{193}Os, which presents few of the difficulties of the other isotopes, the most precise of the previously measured values of the thermal cross section differ from one another by 5–10 standard deviations. As a result, a remeasurement of the Os thermal cross sections and resonance integrals has been undertaken, the results of which are given in the present report.

By observing the γ-ray spectra of the radioisotopes produced in the neutron activation of Os, it has been possible to obtain considerable improvements in the values of the energies and intensities of the γ rays emitted in the ^{185}Os, ^{190}Os^{m}, and ^{193}Os decays, in the corresponding energy levels of the daughters (^{185}Re, ^{190}Os, ^{193}Ir), and in the deduced intensities of the β-decay feedings to levels in ^{185}Re and ^{193}Ir. Those results are included in the present report, along with remeasurements of the decay half-lives of ^{185}Os, ^{190}Os^{m}, ^{191}Os^{g,m}, and ^{193}Os.

II. EXPERIMENTAL DETAILS

Samples of Os metal powder of mass 5–10 mg in natural isotopic abundances were irradiated in the Oregon State University TRIGA reactor. Two different facilities were used: a thermal column (TC, nominal thermal and epithermal fluxes of respectively 8×10^{10} and 2×10^{8} neutrons cm^{-2} s^{-1}) and a fast pneumatic transfer facility ("rabbit," fluxes 1×10^{13} and 3×10^{11} neutrons cm^{-2} s^{-1}). Some rabbit samples were encased in a Cd box of 1 mm wall thickness to isolate the epithermal component. Irradiation times ranged from several minutes in the rabbit to several hours in the TC. Typical activities at end of bombardment were ^{185}Os, 1 kBq; ^{190}Os^{m}, 20 kBq; ^{191}Os, 300 kBq; ^{193}Os, 150 kBq.

All irradiations were accompanied with monitors for the neutron flux determinations. Primary flux monitors were Au and Co as dilute alloys (0.134% and 0.438%, respectively) in thin Al metal foils. Flux determinations were made by assuming the thermal cross section and resonance integral of Au to be, respectively, 98.65 $\pm$ 0.09 b and 1550 $\pm$ 28 b, and those of Co to be 37.18 $\pm$ 0.06 b and 74 $\pm$ 2 b [1]. Zr served as a secondary flux monitor, especially for the determination of the small epithermal component in the TC.

The γ rays were observed with a high-purity Ge detector (nominal volume of 169 cm^3, efficiency of 35% compared with NaI at 1332 keV, resolution of 1.68 keV at 1332 keV). Source-to-detector distances for the cross-section measurements were generally 10 to 20 cm, for which coincidence summing effects are negligible. The signals were analyzed with a digital spectroscopy system connected to a desktop computer. Peak areas of the γ-ray lines, which were well isolated from neighboring peaks, were determined with the ORTEC MAESTRO software [3].

TABLE I. Properties of Os isotopes for neutron irradiation.

Capture process	Abundance (%)	Half-life	Analyzing γ rays Energy in keV and branching ratio in %
184 → 185	0.02(1)	92.95(9) d	646.1 (79.6%)
189 → 190 *m*	16.15(5)	9.86(3) min	186.7 (73.1%), 361.1 (95.3%), 502.6 (97.8%), 616.3 (99.4%)
190 → 191 *m*	26.26(2)	14.99(2) d	129.4 (26.5%)
190 → 191 *g*		13.6(2) h	
192 → 193	40.78(19)	29.830(18) h	321.6 (1.25%), 387.5 (1.23%), 460.5 (3.88%)

Properties of the Os isotopes used for the cross-section determinations are listed in Table I. The isotopic abundances are taken from the current recommended values of the IUPAC Commission on Isotopic Abundances and Atomic Weights [4]. Decay half-lives and γ-ray branching intensities are taken from the present determinations or from the compiled data in the Nuclear Data Sheets [5–8] (NDS) and the online Evaluated Nuclear Structure Data File (ENSDF) compilation [9].

The activities a deduced from measuring the γ-ray intensities were analyzed using the rate equation for a simple capture and decay process, which gives

$$a\,(t) = R(1 - e^{-\lambda t_{\rm i}})e^{-\lambda t}, \tag{1}$$

where a is the activity at time t after the end of the irradiation, R is the reaction rate, and $t_{\rm i}$ is the irradiation time. The reaction rate can be expressed as

$$R = N_0(\sigma\phi_{\rm th} + I\phi_{\rm epi}) \tag{2}$$

where N_0 is the number of target atoms (assumed constant), σ represents the effective thermal cross section, I is the effective resonance integral, and $\phi_{\rm th}$ and $\phi_{\rm epi}$ are the thermal and epithermal fluxes. For irradiations in the thermal column, where the flux is nearly Maxwellian, the effective thermal cross section σ is essentially identical to σ_0, the 2200 m/s cross section (assuming the thermal cross section is proportional to $1/v$). For irradiations in the rabbit (which terminates in the reactor core), the effective σ is larger than σ_0 by about 1.5%, which is within the margin of uncertainty of the present measurement. The effective resonance integral usually exceeds the "true" resonance integral I_0 by a quantity equal to about $0.45\sigma_0$, representing the effect of the tail of the $1/v$ distribution in the resonance region. Since the resonance integral in many cases is an order of magnitude larger than the thermal cross section, this correction is typically about 5%, which is roughly the margin of uncertainty of the present measurements. However, in certain cases of neutron-deficient nuclei in this region (including not only ^{184}Os but also ^{190}Pt and ^{196}Hg), the thermal cross section is much larger than the resonance integral, perhaps to the extent that subtracting $0.45\sigma_0$ from the effective resonance integral would lead to a negative value for the "true" resonance integral. These stable isotopes are of such low abundance that their resonance structure has not been measured, and so it is not known even whether the $1/v$ behavior is at all valid. (For example, a broad low-lying resonance such as that of ^{113}Cd would invalidate this relationship.) Moreover, in calculating the resonance integral, it is generally assumed that the epithermal flux varies as $1/E$; because the epithermal spectrum in different reactor facilities may have different energy dependences, it often may not be possible to compare directly the resonance integrals measured in different facilities.

Equation (1) applies to neutron capture by ^{184,189,192}Os. Capture by ^{190}Os is more complicated, because both the radioactive ground and isomeric states in ^{191}Os are produced. Moreover, it is not possible to observe the isomeric decay directly, because the 74 keV isomeric transition is too weak to be observed among the x-rays that follow the various Os decays. As a result, the 129 keV γ ray from the ground state shows not only the decay of the ground state but also the production of the ground state due to decays of the isomer. Solving the rate equation in this case gives for the ground-state activity following irradiation for a time $t_{\rm i}$:

$$a_g(t_{\rm i}) = -\frac{\lambda_g R_m}{\lambda_m - \lambda_g}(1 - e^{-\lambda_m t_{\rm i}}) + \left(R_g + R_m + \frac{\lambda_g R_m}{\lambda_m - \lambda_g}\right)(1 - e^{-\lambda_g t_{\rm i}}), \tag{3}$$

where R_g and R_m are respectively the reaction rates for direct formation of the ground state and the isomer. At time t following the end of irradiation, the ground-state activity is

$$a_g(t) = \frac{\lambda_g a_m(t_{\rm i})}{\lambda_g - \lambda_m}e^{-\lambda_m t} + \left[a_g(t_{\rm i}) - \frac{\lambda_g a_m(t_{\rm i})}{\lambda_g - \lambda_m}\right]e^{-\lambda_g t}. \tag{4}$$

In a counting interval of duration Δt lasting from $t = t_0$ to $t = t_0 + \Delta t$, the number of counts N_c is determined from the integral of Eq. (4):

$$N_c = \int_{t_0}^{t_0+\Delta t} a_g(t)dt = \frac{\lambda_g a_m(t_{\rm i})}{\lambda_m(\lambda_g - \lambda_m)}e^{-\lambda_m t_0}(1 - e^{-\lambda_m \Delta t}) + \left[\frac{a_g(t_{\rm i})}{\lambda_g} - \frac{a_m(t_{\rm i})}{\lambda_g - \lambda_m}\right]e^{-\lambda_g t_0}(1 - e^{-\lambda_g \Delta t}). \tag{5}$$

Use of Eq. (5) compensates for the increase or decrease in the activity of the source during the counting interval.

The γ-ray spectra were analyzed for peak locations and areas using the fitting code SAMPO [10]. Energy calibrations for the spectroscopy studies were done by counting Os samples simultaneously with samples of ^{133}Ba and ^{152}Eu [11]. From these experiments the energies of the strongest lines in the decays could be determined. These energies were in turn used to determine the energies of the weaker lines in longer runs counting only the Os sources. For isolated peaks with good statistics (generally those with relative intensities above 0.1%), the combined calibration and fitting uncertainties would generally give a net energy uncertainty below 10 eV. To allow

for possible systematic uncertainties, the minimum energy uncertainty has been set at 10 eV.

Efficiency calibrations were done with sources of ^{133}Ba and ^{152}Eu. The calibration below 200 keV was also characterized using reactor-produced sources of ^{160}Tb, ^{169}Yb, and ^{182}Ta. The minimum uncertainty in intensities for the spectroscopic studies has been set at 2% for energies below 200 keV and 1% above 200 keV. This represents primarily the fitting uncertainty in the efficiency calibrations.

III. HALF-LIFE MEASUREMENTS

A. ^{185}Os

The ^{185}Os activity is the longest-lived of the Os radioisotopes produced in neutron capture. The irradiated sample was stored for several months to allow the shorter-lived activities to decay away. At the start of counting, the sample contained 107 kBq of ^{185}Os and also 33 kBq of ^{192}Ir ($t_{1/2} = 73.827$ d), the latter a result of the activation of a small Ir impurity in the Os samples. Figure 1 shows the decay of the 646 keV transition as followed over a period of 150 days. From observation of this line over 1.5 years, the resulting value of the half-life is 92.95 d. The statistical uncertainty in this result is 0.01 d. However, systematic uncertainties in the half-life can often contribute at a level that far exceeds the statistical uncertainty. The principal contributions to the systematic uncertainty are the time variation in the background under the γ-ray peak and the dead-time correction in the acquisition system. Because the only impurity in the sample (^{192}Ir) has a half-life comparable to that of the ^{185}Os and contributes only weakly to the background around 646 keV, the background contribution to the systematic uncertainty is negligibly small. The dead-time contribution was minimized by keeping the dead times small (less than 10%). The dead-time compensation was verified by simultaneous observation of the γ rays from ^{192}Ir. The resulting uncertainty in the half-life is estimated at no greater than 0.1%, and so the final result of the measurement is 92.95 ± 0.09 d, in reasonable agreement with and considerably more precise than the NDS value (93.6 ± 0.5 d), taken from the previous work of Johns *et al.* [12].

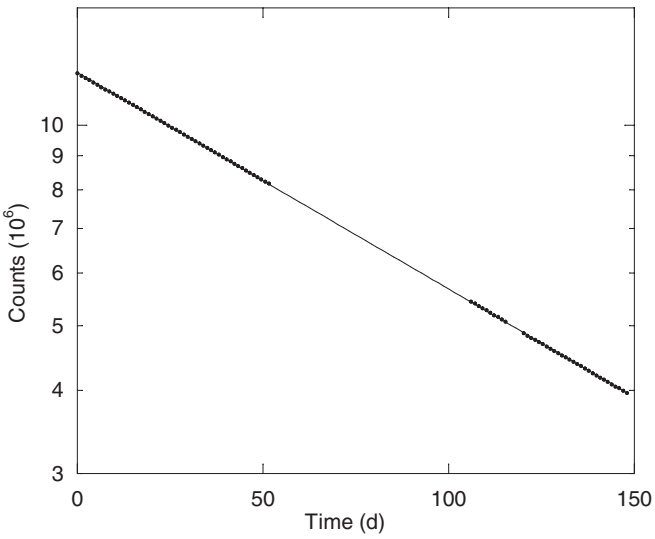

FIG. 1. Time variation of counting rate of the 646 keV line from the ^{185}Os decay. The error bars are smaller than the plotted points.

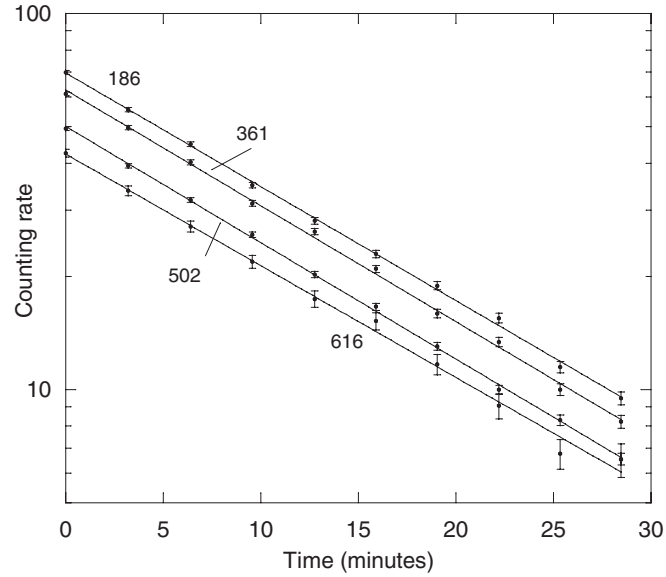

FIG. 2. Counting rates of 4 lines from the ^{190}Os^m decay.

B. ^{190}Os^m

The 4 lines from the ^{190}Os^m decay (186, 316, 502, 616 keV) were followed over approximately 2 to 3 half-lives from 7 different samples. Figure 2 shows results from one sample for the 4 lines. As discussed below, small corrections were applied to the 361 keV line to account for the presence of a weak ^{193}Os line at that energy (initially about 3% of the ^{190}Os^m line) and to the 616 keV line to account for a nearby 617 keV line (initially about 25%) from a ^{80}Br^m impurity present in the irradiated polyethylene vials used for the samples. The weighted average of the 28 individual values (4 lines from each of 7 samples) gives a half-life of 9.86 ± 0.03 min, with a χ^2 per degree of freedom of 1.5. This value for the half-life is in agreement with but more precise than the previous values of 9.9 ± 0.1 min [13] and 9.85 ± 0.14 min [14].

C. ^{191}Os^{g,m}

The ^{191}Os^m metastable state decays with a half-life of 13 h to the 15 d ground state. The half-life of the ground state can be measured directly in a sample in which the population of the metastable state has been thoroughly depleted. Figure 3 shows a set of data for the 129 keV γ ray from the ground-state decay beginning about 15 d after the irradiation and lasting almost 3 half-lives. The fit shows better agreement with a half-life of 15.0 d than the previously accepted value of 15.4 d. The deduced value of the ground-state half-life from several such data sets is $t_{1/2}(g) = 14.99 \pm 0.02$ d. The presently accepted NDS value of 15.4 ± 0.1 d is based on a report by

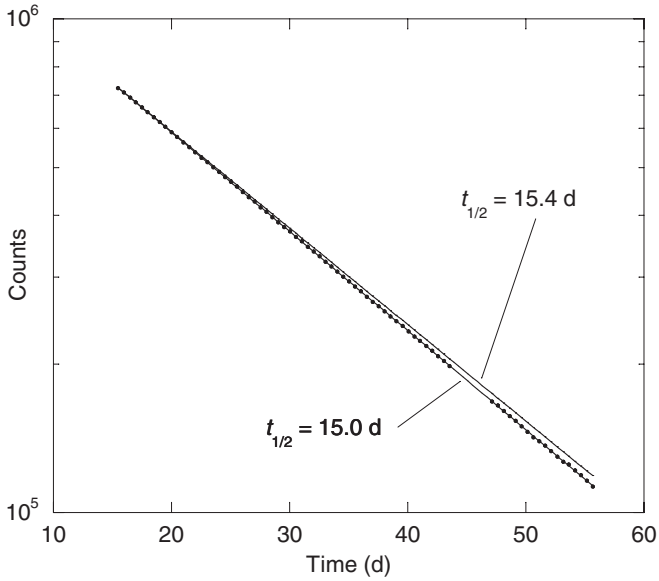

FIG. 3. Counting rate of 129 keV γ ray, showing the exponential decay at long times following the irradiation. The gap in the data was due to an electrical power interruption. The solid lines show the expected behavior for the currently accepted half-life (15.4 d) and for the presently determined value of 15.0 d.

Agin *et al.* [15], but the results of various experiments summarized in the NDS range from about 14.4 to 16.0 d.

The decay of ^{191}Os^m takes place through a highly converted 74 keV $M3 + E4$ isomeric transition with γ branching of only 0.07% [7]. Such a weak transition cannot be observed against the intense background of Ir K_β x-rays of energies 73 to 75 keV. As a result, the decay of the metastable state must be analyzed in the present experiments through its effect in increasing the population of the ground state, which is in turn revealed through the 129 keV γ ray emitted in the ground-state decay. Figure 4 shows the increase in the 129 keV counting rate in data taken about 4.5 h following the end of irradiation.

The value of the half-life can be adjusted until the χ^2 per degree of freedom is minimized. Figure 4 shows the early data with the half-life fixed at the currently accepted value (13.1 h), which gives values of the χ^2 per degree of freedom in the range 7 to 8 for several data runs, and the best fit with the half-life of the isomer as a free parameter, for which the χ^2 per degree of freedom lies between 1 and 2. The overall best fit gives a half-life for the isomer of $t_{1/2}(m) = 13.6 \pm 0.2$ h, which differs by about 2 standard deviations from the currently accepted NDS value, 13.10 ± 0.05 h, based on a measurement of the L x-rays by Campbell and O'Brien [16].

D. ^{193}Os

Figure 5 shows the decay with time of 6 intense lines in the ^{193}Os decay: 139, 280, 322, 387, 460, and 557 + 559 keV (the latter being an incompletely resolved doublet) from one irradiated Os sample. In all the 6 decays were tracked in a total of 6 samples for times ranging from 2.5 to 6 half-lives. For the sample shown in Fig. 5, the 6 lines produced half-life values of, respectively, (in hours) 29.818 ± 0.036 (χ^2 per degree of freedom = 0.78), 29.788 ± 0.089 (1.85), 29.857 ± 0.088 (1.03), 29.977 ± 0.093 (0.43), 29.838 ± 0.046 (1.33), and 29.817 ± 0.079 (0.60). These 6 values overlap nicely, and their weighted average is 29.834 ± 0.024 (0.59). Similar values were obtained from the additional 5 samples, which gave weighted averages for the 6 γ rays of 29.860 ± 0.039 (0.57), 29.814 ± 0.020 (1.50), 29.836 ± 0.024 (2.49), 29.852 ± 0.044 (1.38), and 29.798 ± 0.055 (3.38). The weighted average of the results from all 6 samples is 29.830 ± 0.011 h, where the uncertainty represents only the statistical and fitting contributions.

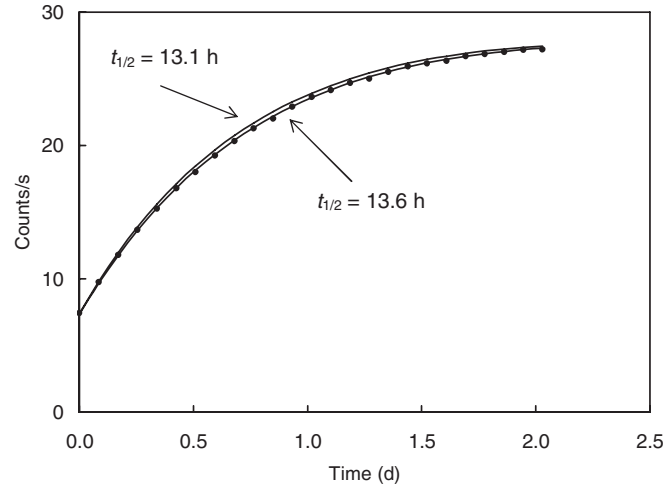

FIG. 4. The 129 keV counting rate at early times. The dots represent the experimental points (error bars are much smaller than the size of the points). The solid lines represent the expected dependence for the currently accepted half-life (13.1 h) and the presently determined value of 13.6 h.

The two principal contributions to the systematic uncertainty are generally the time variation in the background under the γ-ray peaks and the reliability of the dead-time corrections of the counting system. No time variation was observed in the

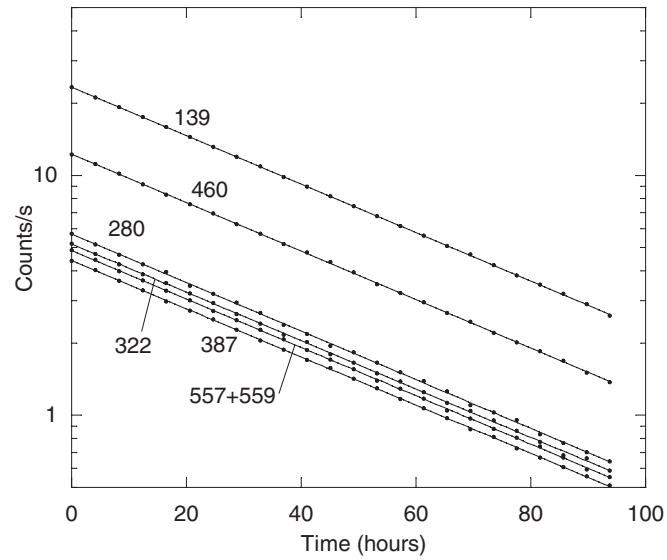

FIG. 5. Time dependence of most intense lines in ^{193}Os decay.

peak backgrounds, and the agreement of the results for the 6 peaks ranging from 139 to 559 keV suggests that background contributions are not contributing significantly relative to the precision of the experiment. The dead-time corrections were minimized by keeping the dead time small in all experiments (less than 10% at the start of counting) and by monitoring long-lived peaks simultaneously with the ^{193}Os peaks. These systematic uncertainties are estimated to be no larger than 0.05%, and so the final result of the present experiments is 29.830 ± 0.018 h.

The presently accepted NDS value for this half-life is 30.11 ± 0.01 h based on a value reported by Antony *et al.* [17]. The reasons for the substantial disagreement between the present result and the previous result are not apparent, but one possibility is discussed below in Sec. VI.

IV. RESULTS OF CROSS-SECTION MEASUREMENTS

A. ^{184}Os$(n,\gamma)^{185}$Os

From the present measurement in the thermal column, the thermal cross section of ^{184}Os was deduced to be 3480 b, and from the Cd-shielded rabbit measurements the effective resonance integral was determined to be 330 b. Assuming the latter value of the resonance integral, the unshielded rabbit gives an effective thermal cross section of 3340 b. Absent the uncertainty in abundance, the uncertainty in the present value of the thermal cross section would be ±150 b and that of the resonance integral would be ±20 b, based primarily on uncertainties in the neutron flux measurements (3%), mass determination (1% to 2%), γ-ray branching (1%), half-life (0.5%), and detector efficiency (1%). However, the principal contribution to the uncertainty of these measurements is that of the natural abundance of ^{184}Os, 0.02% ± 0.01%. This 50% uncertainty in abundance translates into cross section values of $\sigma = 3480^{+3480}_{-1160}$ b and $I = 330^{+330}_{-110}$ b.

The thermal cross section for radiative capture by ^{184}Os has been previously reported by Kim and Adams [18] to be 3005 ± 122 b. In their analysis they used naturally occurring Os with an assumed isotopic abundance of 0.018% but apparently did not include the ±50% uncertainty in the abundance in their determination of the uncertainty of the cross section. De Corte and Simonits [19] report a value of 3613 b, with an uncertainty of ±50% based entirely on the uncertainty in the abundance.

The previously reported measured resonance integrals of ^{184}Os show a large and inexplicable variation. Kim and Adams [18] report a value of $I_0 = 0.38$ b (corrected for the $1/v$ component). Van der Linden *et al.* [20] report $I/\sigma = 0.200 \pm 0.015$, which would lead to a value of the resonance integral (including the $1/v$ contribution) of 750 b. De Corte and Simonits [19] reference an unpublished value for this ratio of 0.43 (no uncertainty given), which would lead to a resonance integral (including the $1/v$ contribution) in the range of 1600 b.

B. ^{189}Os$(n,\gamma)^{190}$Os^m

The ^{189}Os cross sections were obtained by averaging the results for the 4 γ rays listed in Table I. No deviations from the average beyond the branching uncertainties were observed. The average of the results for the Cd-shielded rabbit was $I = 32.9 \pm 1.9$ mb. Using this value to analyze the unshielded rabbit data, the average thermal cross section was determined to be $\sigma = 0.257 \pm 0.018$ mb. Owing to the short half-life, this cross section could not be determined from the thermal column data.

In previous measurements of the thermal cross section leading to ^{190}Os^m, Mangal and Gill [21] report a value of 8 ± 2 mb using natural Os while Tilbury and Wahl [14] report a value of 0.26 ± 0.03 mb from experiments using natural Os and also separated isotopes of both ^{189}Os and ^{190}Os. The present results are in excellent agreement with those of Tilbury and Wahl. Each of these previous experiments suffered from the poor resolution characteristic of scintillation detectors. Indeed, in the results reported by Tilbury and Wahl, the cross sections deduced from the four cascade γ rays emitted by ^{190}Os^m do not agree with one another, the mutual disagreement being as large as a factor of 4. The present results give excellent mutual agreement of the cross sections deduced for the four cascade transitions, after allowing for small corrections for unresolved transitions in the 361.1 and 616.3 keV peaks, as discussed below in Sec. V.

Van der Linden *et al.* [20] report a value of 50.5 ± 5.0 for the ratio I/σ, while the present results give $I/\sigma = 120 \pm 10$, in rather poor agreement with the previous results. Van der Linden *et al.* used the 361 keV transition in the decay of ^{190}Os^m to analyze their data from irradiation of natural Os samples; it is possible that the unresolved 361 keV line from ^{193}Os, in which the ratio I/σ has the much smaller value 2.35, is responsible for the reduction in their value of this ratio relative to the present one.

It is also possible to produce ^{190}Os^m through the reaction ^{190}Os(n,n') reaction by fast neutrons. Indeed, Tilbury and Wahl [14] observed this reaction using separated ^{190}Os and report a cross section of 1.48 mb. The flux of fast neutrons (in excess of 1.7 MeV) in our reactor is negligible in comparison with the epithermal flux, and so it can safely be concluded that the (n,n') reaction gives a negligible contribution to the ^{190}Os^m activity in the present experiments.

C. ^{190}Os$(n,\gamma)^{191}$Os^{g,m}

Because the present method employs the 129 keV transition emitted in the decay of the ^{191}Os ground state to deduce the properties of both ground and metastable states, the growth and decay of the ground-state population must be analyzed to determine simultaneously the cross sections of the ground and metastable states.

Figure 6 shows the counting rate of the 129.4-keV γ ray as a function of the time in a source prepared by irradiation in the thermal column, with the start of counting about 4.5 h after the end of the irradiation. The initial increase in the counting rate is due to the decay of the isomer, while after about 10 d the source shows a simple exponential decay characteristic of the lifetime of the ground state. Equation (5) was used to calculate the expected counting rates, and the ground and metastable thermal cross sections were varied until the χ^2

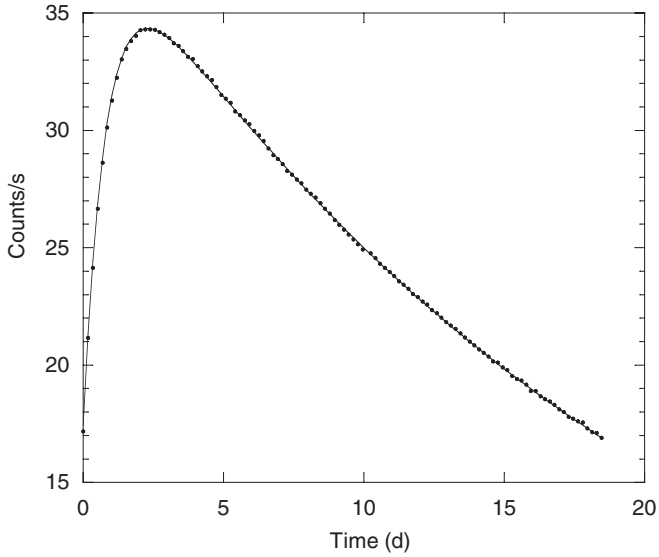

FIG. 6. Fit of thermal column data to determine thermal cross sections for production of ^{191}Os^{g,m}. The solid line is a fit to the data using Eq. (5).

reached a minimum. Figure 6 shows the fitted counting rates with thermal cross sections of 1.96 and 9.04 b respectively for the ground and metastable states. With more than 100 data points taken over 18 days, the fit gives a χ^2 per degree of freedom of 2.7. This fit is minimally sensitive to the resonance integrals because the epithermal flux in the thermal column is very small.

Figure 7 shows a similar fit to the data from the Cd-shielded rabbit experiment, which yields resonance integrals (including the $1/v$ contribution) of 4.77 and 25.4 b respectively for the ground and metastable states. Finally, the unshielded rabbit data produced a similar fit with a sharp minimum for thermal cross sections of respectively 1.89 and 9.01 b for the ground and metastable states and a rather broad minimum (reflecting

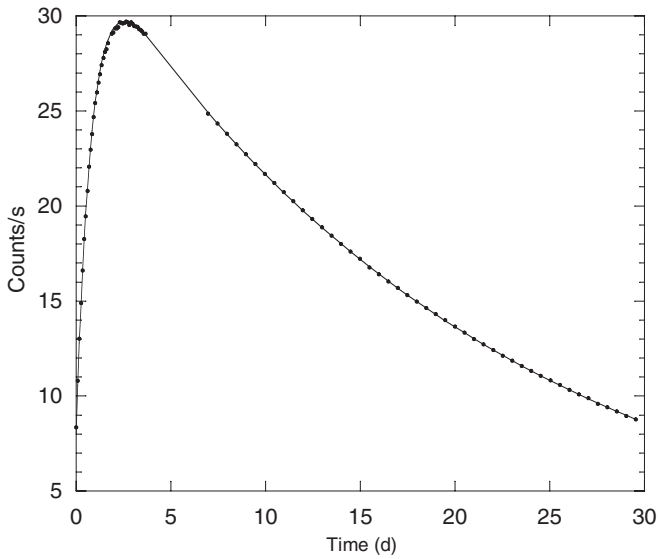

FIG. 7. Fit of Cd-shielded rabbit data to determine resonance integrals for production of ^{191}Os^{g} and ^{191}Os^{m}.

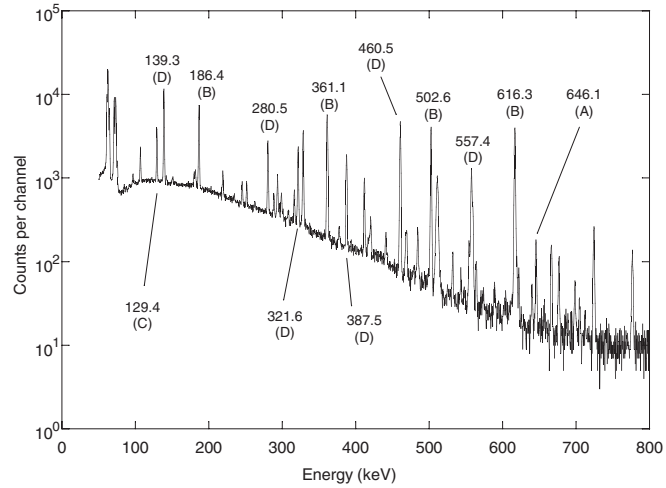

FIG. 8. γ-ray spectrum from decay of Os radioisotopes taken immediately following irradiation. Labeled peaks are from ^{185}Os (A), ^{190}Os^{m} (B), ^{191}Os (C), and ^{193}Os (D).

the relative insensitivity to the small flux of epithermal neutrons) with resonance integrals of respectively 4.63 and 25.6 b.

Taking into account fitting uncertainties, as well as uncertainties in the half-lives, neutron flux, and detector efficiency (branching and abundance uncertainties being negligible in this case), the final result is

$$\sigma(g) = 1.93 \pm 0.10 \text{ b}, \quad I(g) = 4.77 \pm 0.29 \text{ b},$$
$$\sigma(m) = 9.03 \pm 0.49 \text{ b}, \quad I(m) = 25.4 \pm 1.5 \text{ b}.$$

Kim and Adams [18] determined the total $g + m$ thermal cross section and resonance integral from an activation measurement to be respectively 13.2 ± 0.2 b and 23.1 ± 0.5 b, but their analysis used half-life (15.7 d) and branching (25.3%) values that have been superseded by more precise data. Van der Linden *et al.* [20] report 2.44 ± 0.04 and 2.40 ± 0.05 for the ratio of the uncorrected resonance integral to the thermal

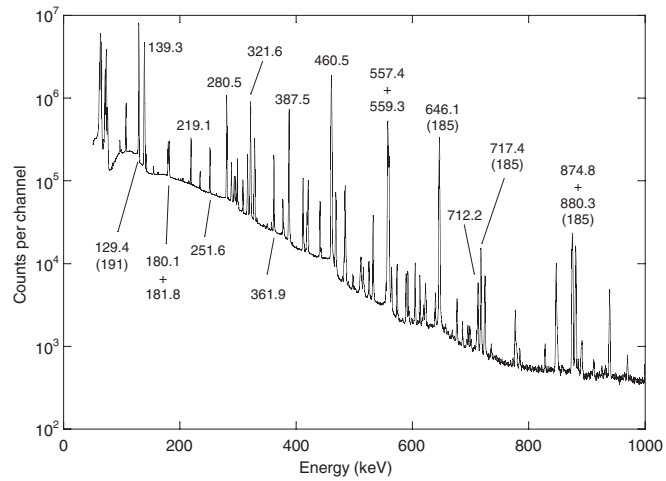

FIG. 9. γ-ray spectrum of Os radioisotopes taken 2 days after irradiation. Peaks not labeled with mass numbers 191 or 185 are from the decay of ^{193}Os.

TABLE II. Energies and intensities of γ rays emitted in decay of ^{185}Os.

Previous work[a]		Present work		Levels[b]	
E (keV)	I	E (keV)	I	Initial	Final
71.313(2)	0.34(14)			*D*	*C*
121.2(1)	0.03(1)			*E*	*C*
125.3581(9)	0.438(15)	125.364(10)	0.442(29)	*B*	*A*
157.7				*F*	*D*
162.852(7)	0.726(22)	162.858(10)	0.759(15)	*G*	*D*
229.1				*F*	*C*
234.157(9)	0.529(13)	234.151(10)	0.545(5)	*G*	*C*
592.074(4)	1.69(3)	592.080(10)	1.69(2)	*D*	*B*
646.116(9)	100(1)	646.127(10)	100(1)	*C*	*A*
717.424(12)	5.05(5)	717.434(10)	5.04(5)	*D*	*A*
749.46(8)	0.0040(5)			*F*	*B*
755				*G*	*B*
768.93(6)	0.0045(4)			*E*	*A*
805.7	0.000 05(4)			*H*	*B*
874.813(13)	8.07(7)	874.830(10)	8.09(8)	*F*	*A*
880.523(13)	6.63(8)	880.287(10)	6.62(7)	*G*	*A*
931.057(15)	0.062(2)	931.030(32)	0.062(2)	*H*	*A*

[a]From NDS and ENSDF compilations [5,9].
[b]See Table III for identification of levels.

cross section for the ground and metastable states, while the present values give ratios of 2.47 ± 0.19 and 2.81 ± 0.23, in acceptable agreement with the former values.

D. ^{192}Os$(n,\gamma)^{193}$Os

The cross sections for capture by ^{192}Os were determined by following the decays of the 322, 387, and 460 keV lines from the ^{193}Os decay. Nine samples were irradiated: 2 in the thermal column, 4 in the unshielded rabbit, and 3 in the Cd-shielded rabbit. Analysis of the latter samples gave an uncorrected resonance integral of 7.45 b. The TC and unshielded rabbit samples yielded a thermal cross section of 3.19 b. Determining the uncertainty of the results gives

$$\sigma = 3.19 \pm 0.16 \text{ b}, \quad I = 7.45 \pm 0.45 \text{ b}.$$

Kim and Adams [18] report 2.0 ± 0.1 b for the thermal cross section and 4.5 ± 0.3 b for the corrected resonance integral, while De Corte and Simonits [19] report a value of 3.12 ± 0.15 b for the thermal cross section, in much better agreement with the present result. Van der Linden *et al*. [20] determined the ratio between the uncorrected resonance integral and the thermal cross section to be 2.25 ± 0.06, in excellent agreement with the present value of 2.34 ± 0.18.

V. γ-RAY SPECTROSCOPY

Figure 8 shows a γ-ray spectrum of an irradiated Os sample taken soon after the irradiation, and Fig. 9 shows a two-day spectrum begun after the short-lived ^{190}Os^{m} had decayed away. In addition to ^{185,191,193}Os, this spectrum shows lines from several 6th period transition metals that are present as impurities in Os, including Hf, W, Ta, Ir, and Au, but not Re or Pt. Lines from activated Ru, which is chemically very similar to Os, are also present. The ^{192,194}Ir lines served as additional

TABLE III. Energy levels of ^{185}Re populated in decay of ^{185}Os.

Level	Previous Work[a]				Present Work		
	E (keV)	J^{π}	I_{ε}	Log ft	E (keV)	I_{ε}	Log ft
A	0.000	$5/2^{+}$	<8	>9.8	0.000		
B	125.3587(9)	$7/2^{+}$			125.364(10)		
C	646.134(4)	$1/2^{+}$	77(3)	7.32(2)	646.128(10)	80.6(2)	7.293(2)
D	717.446(4)	$3/2^{+}$	5.0(4)	8.28(4)	717.440(8)	5.12(6)	8.261(6)
E	768.93(6)	$(5/2^{+})$	0.07(2)	9.15(15)			
F	874.815(13)	$3/2^{+}$	6.4(3)	7.26(3)	874.832(10)	6.68(8)	7.212(7)
G	880.331(6)	$1/2^{+}$	7.1(3)	7.15(3)	880.289(8)	7.51(8)	7.103(7)
H	931.063(20)	$(3/2)^{+}$	0.0521(12)	7.62(3)	931.032(32)	0.0511(17)	8.507(17)

[a]From NDS and ENSDF compilations [5,9].

TABLE IV. Energies and intensities of γ rays emitted in decay of $^{190}Os^m$.

Previous work			Present work		Levels[c]	
E (keV)[a]	I[a]	E (keV)[b]	E (keV)	I	Initial	Final
38.9(1)	0.081(3)				F	E
186.7(1)	70.2(6)	186.718(2)	186.720(10)	73.1(20)	B	A
361.2(1)	94.88(10)	361.136(6)	361.121(14)	95.3(15)	C	B
502.5(1)	97.79(5)	502.6(3)	502.578(10)	97.8(10)	D	C
616.5(1)	98.62(3)		616.342(15)	99.4(20)	E	D

[a]From NDS decay compilation [6]; expected γ-ray intensities deduced from observed or calculated internal conversion intensities.
[b]From n,γ study by Casten *et al.* [26].
[c]See Table V for identification of levels.

calibrations for the determination of the energies of the Os lines.

A. ^{185}Os decay

The energies and intensities of the γ rays observed in the decay of ^{185}Os to ^{185}Re are shown in Table II and compared with the currently accepted values from the NDS [5], which are based on previous spectroscopic studies of the ^{185}Os decay by Brenner *et al.* [22] and Goswamy *et al.* [23]. The agreement is excellent, with the exception of the 880.287 keV transition. The previous value of 880.523 keV, taken from Brenner *et al.*, is very likely in error, as the resulting identical energy assigned by them to the corresponding excited state does not agree with the placement of the other two transitions that depopulate that state. A later report by Meyer [24] gives a different value (880.290 $\pm$ 0.006 keV) in better agreement with the present value, as does a comprehensive study of γ-ray calibration standards by Helmer and van der Leun [11] (880.2816 $\pm$ 0.0027 keV).

Table III shows the corresponding energy levels in ^{185}Re deduced from the ^{185}Os γ rays in the present work compared with the NDS values. Again, there is rather poor agreement for the 880.289 keV level, for which the NDS value may have been influenced by the high value of their recommended energy of the ground-state transition. By comparing the total transition intensity (γ plus internal conversion electron) populating and depopulating each level, the β-feeding intensities have been deduced, along with the corresponding log ft values. In this calculation it has been assumed that there is negligible direct β feeding corresponding to the unique first-forbidden decay from the $1/2^-$ ^{185}Os to the $5/2^+$ ground state of ^{185}Re, as is the case in the otherwise similar decays of ^{181}Os and ^{183}Os.

B. $^{190}Os^m$ decay

No previous γ-ray spectroscopic determination of the energies and intensities of the γ rays emitted in the $^{190}Os^m$ decay using Ge detectors has been reported, although the transition energies have been determined by Harmatz and Handley [25] from the conversion electrons emitted in the decay, and the γ-ray intensities have been inferred from the conversion coefficients assuming a direct cascade of four $E2$ radiations. These intensity values are shown in Table IV, along with the transition energies deduced from the conversion electron study. Precise energies of the two lowest members of the cascade have been determined by Casten *et al.* [26] from a measurement of the primary and secondary γ rays following neutron capture; their values are included in Table IV.

The energies and intensities deduced from the present work (normalized so that the 502.6 keV line has intensity 97.79, based on the internal conversion coefficient) are shown in Table IV, and the corresponding deduced energy levels are given in Table V. The 186.7 and 502.6 keV peaks are well isolated in the γ-ray spectra, but the 361.1 keV and 616.3 keV peaks have small additional contributions that could not be completely resolved in the peak fitting. The 361.1 keV peak includes the 361.9 keV line from the decay of ^{193}Os; the intensity of this competing line typically amounted to 5% to 10% of the intensity of the $^{190}Os^m$ line during the first two half-lives of the $^{190}Os^m$ decay. The 616.3 keV line includes a small impurity from the 616.8 keV line in the decay of $^{80}Br^m$, which is present as an impurity in the polyethylene vials used to encapsulate samples for reactor irradiations. Using the relative intensity of the 616.8 and 666.3 keV lines from the Br decay [27], the impurity intensity could be precisely determined. This impurity amounted to 20% to 40% of the intensity of the $^{190}Os^m$ line during the first two half-lives of the $^{190}Os^m$ decay and contributed to a slight increase in the deduced uncertainties of the energy and intensity of the 616.3 keV Os line.

C. ^{193}Os decay

The decay of ^{193}Os is the most complex of the Os radioisotopes produced by neutron activation, with more than

TABLE V. Energy levels of ^{190}Os populated in decay of $^{190}Os^m$.

Level	Previous Work[a]		Present Work
	E (keV)	J^π	E (keV)
A	0.000	0^+	0.000
B	186.718(2)	2^+	186.720(10)
C	547.854(7)	4^+	547.841(17)
D	1050.38(7)	$(6)^+$	1050.420(20)
E	1666.47(15)	$(8)^+$	1666.763(25)
F	1705.4(2)	$(10)^-$	1705.66(10)

[a]From NDS compilation [6].

TABLE VI. Energies and intensities of γ rays emitted in decay of ^{193}Os.

Previous decay studies[a]		In beam[b]	Present work		Levels[c]	
E (keV)	I	E (keV)	E (keV)	I	Initial	Final
41.18(7)		41.219(13)			*E*	*D*
65.87(6)	0.06					
73.029(15)	82(12)	73.050(22)	72.951(46)	74(14)	*B*	*A*
80.240(6)		80.236(7)			*C*	*A*
96.84(3)	2.5(2)		96.815(15)	2.42(5)	*J*	*I*
98.75(5)	0.42(6)		98.681(15)	0.423(10)	*I*	*H*
107.009(13)	14.5(16)	107.022(5)	107.019(10)	14.6(3)	*E*	*B*
136	0.011(3)	135.880(29)			*M*	*K*
138.92(3)	97.8(18)	138.938(5)	138.932(10)	99.1(19)	*D*	*A*
142.132(17)	1.65(25)	142.159(3)	142.139(10)	1.72(3)	*O*	*L*
154.74(3)	0.67(6)	154.721(4)	154.808(10)	0.692(13)	*N*	*J*
180.05(3)	4.6(4)	180.071(7)	180.061(10)	4.31(8)	*E*	*A*
181	0.008				*O*	*K*
181.83(3)	4.8(4)	181.792(7)	181.785(10)	4.63(9)	*H*	*E*
197.4(2)	0.12(4)		197.486(24)	0.110(6)	*K*	*H*
201.5(3)	0.07(4)	201.535(7)	201.521(45)	0.097(9)	*K*	*G*
219	0.22(5)	218.826(2)			*G*	*D*
219.14(4)	6.8(4)	219.158(7)	219.144(10)	6.58(11)	*F*	*C*
234.58(5)	1.23(9)	234.608(7)	234.572(10)	1.23(3)	*M*	*I*
251.63(4)	5.5(3)	251.635(7)	251.645(10)	5.34(7)	*N*	*I*
280.446(22)	31.71(20)	280.465(3)	280.482(10)	31.9(3)	*I*	*E*
288.81(5)	3.80(21)	288.807(9)	288.819(10)	3.62(4)	*H*	*B*
290	0.012				*Q*	*K*
298.82(5)	4.76(24)	298.828(10)	298.831(10)	4.79(5)	*L*	*F*
317	0.026(7)				*R*	*J*
321.590(22)	32.23(20)	321.604(7)	321.616(10)	31.9(3)	*I*	*D*
333.15(21)	0.046(18)	333.275(36)	333.247(53)	0.067(5)	*M*	*H*
337.7(5)	0.03(2)	337.332(27)	337.302(73)	0.017(3)	*M*	*G*
350.20(17)	0.17(4)	350.325(9)	350.343(16)	0.138(4)	*N*	*H*
357.73(17)	0.26(7)	357.765(52)	357.761(12)	0.233(4)	*G*	*A*
361.83(7)	6.7(3)	361.860(15)	361.858(10)	7.30(7)	*H*	*A*
377.34(7)	1.75(14)		377.340(10)	1.67(2)	*J*	*E*
378	0.041(10)	378.533(8)	378.379(102)	0.04(1)	*O*	*H*
379.04(14)	0.27(6)	379.230(11)	379.194(31)	0.26(1)	*K*	*E*
387.48(3)	31.77(20)	387.520(18)	387.509(10)	31.3(3)	*I*	*B*
413.86(17)	0.114(24)	413.756(8)	413.729(16)	0.105(5)	*R*	*I*
418	0.18(4)				*L*	*E*
418.32(7)	1.45(11)	418.480(37)	418.431(16)	1.34(1)	*J*	*D*
420.29(5)	4.02(24)	420.351(8)	420.346(10)	4.07(4)	*K*	*D*
440.95(5)	2.27(12)	440.980(13)	440.986(19)	2.27(2)	*O*	*F*
460.50(3)	100.0(5)	460.547(7)	460.547(10)	100(1)	*I*	*A*
484.25(5)	4.4(3)	484.323(12)	484.359(10)	4.33(6)	*J*	*B*
486.11(15)	0.29(14)	486.274(11)	486.255(10)	0.271(3)	*K*	*B*
512.3(3)	0.04(2)				*R*	*H*
515.00(9)	0.33(4)	515.064(9)	515.064(10)	0.293(4)	*M*	*E*
516.3(4)	0.06(3)	516.475(15)	516.524(38)	0.073(2)	*R*	*G*
525.02(7)	0.40(3)	525.163(49)	525.190(10)	0.414(4)	*L*	*B*
532.04(5)	2.14(12)	532.127(18)	532.126(10)	2.14(2)	*N*	*E*
556	0.08(2)	556.175(9)			*M*	*D*
557.37(7)	35(3)	557.429(21)	557.401(10)	33.7(3)	*J*	*A*
559.25(7)	13.2(10)	559.288(39)	559.289(10)	12.4(1)	*K*	*A*
560	0.07(2)	560.327(28)			*O*	*E*
573.34(9)	0.51(4)	573.213(56)	573.267(10)	0.519(5)	*N*	*D*
598.28(24)	0.018(6)		598.438(78)	0.018(2)	*L*	*A*
639.13(9)	0.200(21)		639.151(10)	0.197(2)	*N*	*B*

TABLE VI. (*Continued.*)

Previous decay studies[a]		In beam[b]	Present work		Levels[c]	
E (keV)	I	E (keV)	E (keV)	I	Initial	Final
667.7(3)	0.024(7)	667.963(9)	668.147(55)	0.026(1)	*P*	*D*
695.16(9)	0.078(11)		695.159(14)	0.068(2)	*M*	*A*
709.94(14)	0.048(11)		709.904(27)	0.053(2)	*Q*	*D*
712.10(9)	0.45(4)		712.188(10)	0.431(4)	*N*	*A*
735.37(24)	0.029(5)		735.322(29)	0.027(1)	*R*	*D*
775.9(3)	0.010(5)				*Q*	*B*
778.35(14)	0.045(8)		778.513(14)	0.047(1)	*T*	*F*
784.20(18)	0.017(4)		784.447(56)	0.017(2)	*S*	*E*
800.9(3)	0.008(4)				*R*	*B*
848.86(14)	0.115(14)		848.944(16)	0.114(3)	*Q*	*A*
874.33(13)	0.54(5)		874.306(25)	0.46(3)	*R*	*A*
891.23(14)	0.076(88)		891.340(31)	0.067(3)	*S*	*B*

[a]From NDS compilation [8].
[b]From Drissi [32].
[c]See Table VII for identification of levels.

60 γ rays currently placed in the ^{193}Ir level scheme. The present results for the γ rays emitted in the ^{193}Os decay, which are based on an average of three different samples each counted for at least 2 half-lives, are listed in Table VI, along with the consensus energies and intensities from the NDS [8] and ENSDF [9], which are based on the previous work of Berg and Malmskog [28], Ludington and Raeside [29], Price and Johns [30], and Marnada *et al*. [31]. Also shown in Table VI are the overlapping results from an in-beam study of the ^{193}Ir transitions by Drissi [32]. The present results represent a significant improvement over the previous decay studies, often by an order of magnitude or more in energy and intensity, and the agreement between the present results and the precise energies from the in-beam work is also excellent. Some of the very weak transitions, especially those whose energies overlap stronger transitions, were observed in the previously referenced decay studies as well as in a more recent study by Zahn *et al*. [33] only through coincidence measurements and so could not be confirmed in the present work in singles mode.

TABLE VII. Energy levels of ^{193}Ir populated in the decay of ^{193}Os.

Level	Previous Work[a]				Present Work		
	E (keV)	J^π	I_β (%)	Log ft	E (keV)	I_β (%)	Log ft
A	0.000	$3/2^+$	57(4)	7.48(3)	0.000	57(4)[a]	7.47(3)
B	73.045(5)	$1/2^+$	18(4)	7.87(10)	73.042(6)	16.3(26)	7.92(9)
C	80.239(6)	$11/2^-$					
D	138.940(6)	$5/2^+$	10.9(4)	7.991(17)	138.932(10)	11.6(11)	7.96(5)
E	180.067(5)	$3/2^+$	1.7(4)	8.73(11)	180.062(7)	1.77(17)	8.71(5)
F	299.399(7)	$7/2^-$	0.031(23)	10.3(4)	299.383(12)	0.198(19)	10.47(5)
G	357.768(6)	$7/2^+$	0.017(6)	10.76(16)	357.761(13)	0.0147(14)	10.80(4)
H	361.856(5)	$5/2^+$	0.72(5)	8.79(3)	361.857(6)	0.77(7)	8.75(4)
I	460.535(5)	$3/2^+$	7.74(13)	7.552(9)	460.548(5)	8.2(8)	7.52(5)
J	557.446(7)	$(1/2)^+$	2.45(15)	7.82(3)	557.392(6)	2.5(2)	7.81(4)
K	559.299(6)	$5/2^+$	0.75(5)	8.33(3)	559.294(6)	0.76(7)	8.33(4)
L	598.230(8)	$3/2^-$	<0.02	>9.8	598.231(9)	0.0066(6)	10.29(4)
M	695.133(6)	$5/2^+$	0.099(7)	8.83(4)	695.138(6)	0.104(10)	8.80(5)
N	712.170(7)	$3/2^+$	0.527(21)	8.045(19)	712.195(5)	0.55(5)	8.02(4)
O	740.381(7)	$5/2^-$	0.31(4)	8.18(6)	740.370(12)	0.34(3)	8.14(4)
P	806.902(9)	$(5/2)^+$			807.080(56)	0.00106(10)	10.39(5)
Q	848.93(6)	$5/2^+$	0.0074(8)	9.36(5)	848.920(14)	0.0080(8)	9.32(5)
R	874.291(9)	$3/2^+$,$5/2^+$	0.033(3)	8.58(5)	874.272(14)	0.031(3)	8.61(5)
S	964.43(7)	$1/2^+$	0.0037(4)	8.96(5)	964.416(27)	0.0035(3)	8.99(5)
T	1077.93(9)	$(3/2^-,5/2^-)$			1077.898(16)	0.0020(2)	7.86(7)

[a]From NDS compilation [8].

TABLE VIII. Relative intensities of ^{193}Ir γ rays.

Level energy	γ -ray energies	Relative γ-ray intensity		
(keV)	(keV)	Present work	Marnada *et al.*[31]	Drissi[32]
180.1	180.1	29.5(6)	28.1(17)	28.6(18)
	107.1	100(2)	100(1)	100(4)
357.8	357.8	100(2)	100(30)	100(8)
	218.8		90(20)	27.0(19)
361.9	361.9	100(1)	100(1)	100(8)
	288.8	49.5(5)	49.1(7)	49.0(46)
	181.8	63.4(12)	61.8(35)	79.0(74)
460.5	460.5	100(1)	100.0(5)	100(7)
	387.5	31.3(3)	31.8(2)	28.3(54)
	321.6	31.9(3)	32.2(2)	32.9(38)
	280.5	31.9(3)	31.7(2)	34.9(37)
	98.7	0.42(1)	0.42(10)	
557.4	557.4	100(1)	100(9)	100(10)
	484.4	12.8(2)	13.1(9)	14(3)
	418.4	3.98(3)	4.2(4)	9(2)
	377.3	4.96(6)	5.4(6)	
	96.8	7.18(15)	7.6(6)	
559.3	559.3	100(1)	100(10)	100(8)
	486.3	2.18(2)	2.3(11)	3.0(5)
	420.3	32.8(3)	34.2(25)	36.6(35)
	379.2	2.10(8)	3.0(8)	3.4(5)
	201.5	0.78(7)	0.57(32)	0.9(3)
	197.5	0.89(5)	0.97(32)	
598.2	598.4	0.38(4)	0.38(16)	
	525.2	8.64(8)	8.2(11)	12.0(16)
	418.1		3.8(11)	
	298.8	100(1)	100(1)	100(9)
695.1	695.1	5.5(2)	5.4(10)	
	556.2		6.0(15)	11(1)
	515.1	23.8(3)	21.1(38)	56.6(62)
	337.3	1.4(2)	2.3(15)	181(16)
	333.2	5.4(4)	5.2(29)	11(3)
	234.6	100(2)	100(4)	100(10)
	135.9		0.77(19)	5.3(9)
712.2	712.2	8.07(8)	7.0(9)	
	639.2	3.69(4)	3.3(5)	
	573.3	9.72(10)	8.9(9)	16.9(51)
	532.1	40.1(4)	38.8(5)	40.7(55)
	350.3	2.58(8)	3.3(9)	69(11)
	251.6	100(1)	100(1)	100(5)
	154.8	13.0(2)	13.6(9)	15.3(68)
740.4	601.5			16.3(33)
	560.3		3.0(9)	30.4(50)
	441.0	100(1)	100(2)	100(9)
	378.5	1.8(4)	1.8(4)	2.0(4)
	181.1			
	142.1	75.8(13)	73(6)	71.4(86)

Level energies in ^{193}Ir determined from the present set of γ-ray energies are shown in Table VII. Comparing the uncertainties of the γ-ray energies with the uncertainties in the deduced level energies, 40 of the 53 transitions (75%) agree within one standard deviation and 51 (96%) within two standard deviations, which closely matches the normal distribution and suggests that the uncertainties in the level energies have been neither overestimated nor underestimated relative to the uncertainties in the transition energies. The only substantial difference between the presently deduced level energies and the recommended NDS values is in the case of the 557.392 keV level, for which the NDS value is 557.446 keV.

The 5 transitions depopulating that level as observed in the present work constitute a consistent set yielding level energies between 557.36 and 557.40 keV with a χ^2 per degree of freedom of 2.4.

Table VII also shows the β intensities and corresponding log ft values deduced from the present γ-ray intensities, assuming the ground-state β intensity of 57% from the NDS [8]. The principal contributor to the uncertainty in the β intensities is the uncertainty in the intensity of the 73 keV γ ray (which produces a corresponding uncertainty in the intensity of the ground-state β branch). Overall the β intensities are in good agreement with the previous NDS values and also with the values deduced by Marnada *et al.* [31] from a $\beta\gamma$ coincidence experiment.

VI. DISCUSSION

The present work has resulted in a considerable improvement of the previously available data sets for three properties associated with the decays of the Os radioisotopes: decay half-lives, neutron capture cross sections, and γ-ray spectroscopy. The spectroscopy results lead to a significant improvement in the data sets for the energies and intensities of the decay γ rays and include high-resolution measurement of the γ radiations from ^{190}Os^m.

A comprehensive set of high-resolution γ-ray intensities allows comparison of decay and reaction studies to identify possible misplacements of transitions in the level scheme. Table VIII shows such a comparison for the ^{193}Ir γ rays. The γ-ray intensities are separately normalized so that the strongest transition from each level is given intensity 100. The decay and reaction studies agree very well for the levels up to 598.2 keV, but there are several disagreements for the higher-lying levels. The relative intensities from the decay and reaction studies disagree for all of the transitions from the 695.1 keV level, as well as for the 350.3 keV transition from the 712.2 keV level and the 560.3 and 601.5 keV transitions from the 740.4 keV level. For example, the transition at 601.5 keV observed in the reaction study with intensity equal to 1/6 that of 441.0 keV (i.e., equivalent to about 0.4 units relative to 460.5 keV in the radioactive decay) should have been obvious in the decay spectra but is not present. These disagreements suggest incorrect assignments for these transitions in the reaction study.

The half-life values from the present experiments for ^{185}Os and ^{190}Os^m agree with but are significantly more precise than the previously accepted values. The present values for the half-lives of ^{191}Os^g and ^{193}Os differ significantly from the accepted values measured respectively by Agin *et al.* [15] and Antony *et al.* [17]. It is noteworthy that in both cases the previous half-lives are greater than the present values. Such results have been simulated in the present experiments by using strong sources (with dead times of order 30%) and no external dead-time monitor (such as a long-lived source or a reference pulser). In such cases the high count rates and large dead times early in the life of the radioactive source may result in loss of counts due to inadequate dead-time compensation, with the smaller count rates at the beginning of the decay period giving a longer deduced half-life, typically 0.1% to 1% greater than the half-life obtained with weaker sources and dead-time monitors. Because the previous papers do not discuss correction for dead-time compensation errors, it is not possible to determine whether this effect could be responsible for the differences between the present and previous results.

The present results for the ^{190}Os cross sections leading to the ground and metastable states, deduced simultaneously by fitting the time dependence of the decay of the ground state, are in reasonably good agreement with the results of previous activation experiments. However, they disagree with the result of experiments to deduce the cross section from the intensity of primary γ rays deexciting the capture state, as summarized by Firestone *et al.* [34]. The analysis of the primary γ rays leads to $\sigma(g) = 0.85 \pm 0.04$ b and $\sigma(m) = 16.6 \pm 1.1$ b, which disagree substantially from the present values. The primary γ rays yield for ^{184}Os $\sigma = 4410 \pm 60$ b (not including the 50% uncertainty in abundance) and for ^{192}Os $\sigma = 2.69 \pm 0.12$ b, which also disagree with the present activation values but by a smaller amount than the ^{190}Os cross sections. Accounting for these discrepancies is essential to understanding the neutron capture process in Os, which in turn has important implications for astrophysical processes [35,36]. Of course, cross sections below 1 eV do not play a significant role in the astrophysical processes, but a comprehensive understanding of neutron capture in Os must include analysis of both low-energy and high-energy processes.

ACKNOWLEDGMENTS

The support of the reactor operations staff of the Oregon State TRIGA Reactor in carrying out the irradiations is acknowledged with appreciation.

[1] S. F. Mughabghab, *Atlas of Neutron Resonances: Resonance Parameters and Thermal Cross Sections Z = 1–100* (Elsevier, Amsterdam, 2006).
[2] EXFOR/CSISRS Experimental Nuclear Reaction Data, National Nuclear Data Center, Brookhaven National Laboratory [http://www.nndc.bnl.gov/exfor/exfor00.htm].
[3] ORTEC, Inc. http://www.ortec-online.com/pdf/a65.pdf.
[4] M. Berglund and M. E. Wieser, Pure Appl. Chem. **83**, 397 (2011).
[5] S.-C. Wu, Nucl. Data Sheets **106**, 619 (2005).
[6] B. Singh, Nucl. Data Sheets **99**, 275 (2003).
[7] V. R. Vanin, N. L. Maidana, R. M. Castro, E. Achterberg, O. A. Capurro, and G. V. Marti, Nucl. Data Sheets **108**, 2393 (2007).
[8] E. Achterberg, O. A. Capurro, G. V. Marti, V. R. Vanin, and R. M. Castro, Nucl. Data Sheets **107**, 1 (2006).
[9] Evaluated Nuclear Structure Data File, National Nuclear Data Center, Brookhaven National Laboratory [http://www.nndc.bnl.gov/ensdf/].

[10] P. A. Aarnio, J. T. Routti, and J. V. Sandberg, J. Radiol. Nucl. Chem. **124**, 457 (1988).
[11] R. G. Helmer and C. van der Leun, Nucl. Instrum. Methods Phys. Res., Sect. A **450**, 35 (2000).
[12] M. W. Johns, S. V. Nablo, and W. J. King, Can. J. Phys. **35**, 1159 (1957).
[13] G. Scharff-Goldhaber, D. E. Alburger, G. Harbottle, and M. McKeown, Phys. Rev. **111**, 913 (1958).
[14] R. S. Tilbury and W. H. Wahl, Bull. Am. Phys. Soc. **9**, 664 (1964); H. Arino *et al*., US Atomic Energy Commission Report NYO-10175 (1964).
[15] G. P. Agin, G. E. Clark, C. E. Mandeville, and V. R. Potnis, Nuovo Cimento B **52**, 220 (1967).
[16] J. L. Campbell and P. O'Brien, Nucl. Phys. A **240**, 1 (1975).
[17] M. S. Antony, D. Oster, and A. Hachem, J. Radiol. Nucl. Chem. **164**, 303 (1992).
[18] J. I. Kim and F. Adams, Radiochim. Acta **9**, 61 (1968).
[19] F. De Corte and A. Simonits, J. Radiol. Nucl. Chem. **133**, 43 (1989).
[20] R. Van der Linden, F. De Corte, and J. Hoste, J. Radioanal. Chem. **20**, 695 (1974).
[21] S. K. Mangal and P. S. Gill, Nucl. Phys. **36**, 542 (1962).
[22] D. S. Brenner, M. Lindner, and R. A. Meyer, Phys. Rev. C **16**, 747 (1977).
[23] J. Goswamy, B. Chand, D. Mehta, N. Singh, and P. N. Trehan, Appl. Rad. Isot. **42**, 1033 (1991).
[24] R. A. Meyer, Fizika **22**, 153 (1990).
[25] B. Harmatz and T. H. Handley, Nucl. Phys. **56**, 1 (1964).
[26] R. F. Casten, M. R. MacPhail, W. R. Kane, D. Breitig, K. Schreckenbach, and J. A. Cizewski, Nucl. Phys. A **316**, 61 (1979).
[27] K. S. Krane, Applied Radiation and Isotopes **69**, 201 (2011).
[28] V. Berg and S. G. Malmskog, Nucl. Phys. A **143**, 177 (1970).
[29] M. A. Ludington and D. E. Raeside, Nucl. Instrum. Methods **94**, 193 (1971).
[30] R. H. Price and M. W. Johns, Nucl. Phys. A **187**, 641 (1972).
[31] N. Marnada, H. Miyahara, N. Ueda, K. Ikeda, and N. Hayashi, Nucl. Instrum. Methods Phys. Res., Sect. A **480**, 591 (2002).
[32] S.-E. Drissi, Nucl. Phys. A **621**, 655 (1997).
[33] G. S. Zahn, F. A. Genezini, C. B. Zamboni, and M. T. F. da Cruz, Nucl. Instrum. Methods Phys. Res., Sect. A **605**, 339 (2008).
[34] R. B. Firestone, S. F. Mughabghab, and G. L. Molnár, in *Database of Prompt Gamma Rays from Slow Neutron Capture for Elemental Analysis* (IAEA, Vienna, 2007), Chap. 5.
[35] J. C. Browne and B. L. Berman, Phys. Rev. C **23**, 1434 (1981).
[36] J. Marganiec, I. Dillmann, C. Domingo Pardo, F. Käppeler, and S. Walter, Phys. Rev. C **82**, 035806 (2010).